Title

RNA-Seq reveals placental growth factor regulates the human retinal endothelial cell barrier integrity by transforming growth factor (TGF-β) signaling.

Journal

Enzymologia, 475(1-2)

Authors

Huang, Hu
Saddala, Madhu
Lennikov, Anton
et al.

Publication Date

2020-12-01

DOI

10.1007/s11010-020-03862-z

Peer reviewed

HHS Public Access

Author manuscript

Mol Cell Biochem. Author manuscript; available in PMC 2021 December 01.

Published in final edited form as:

Mol Cell Biochem. 2020 December ; 475(1-2): 93–106. doi:10.1007/s11010-020-03862-z.

RNA-Seq reveals placental growth factor regulates the human retinal endothelial cell barrier integrity by transforming growth factor (TGF-β) signaling

Hu Huang[1,*], **Madhu Sudhana Saddala**[1], **Anton Lennikov**[1], **Anthony Mukwaya**[2], **Lijuan Fan**[1]

[1]The University of Missouri, Columbia, Missouri, United States of America.

[2]Department of Ophthalmology, Institute for Clinical and Experimental Medicine, Faculty of Health Sciences, Linköping University, Linköping, Sweden.

Abstract

Placental growth factor (PlGF or PGF) is a member of the VEGF (vascular endothelial growth factor) family. It plays a pathological role in inflammation, vascular permeability, and pathological angiogenesis. The molecular signaling by which PlGF mediates its effects in nonproliferative diabetic retinopathy (DR) remains elusive. This study aims to characterize the transcriptome changes of human retinal endothelial cells (HRECs) with the presence and the absence of PlGF signaling. Primary HRECs were treated with the PlGF antibody (ab) to block its activity. The total RNA was isolated and subjected to deep sequencing to quantify the transcripts and their changes in both groups. We performed transcriptome-wide analysis, gene ontology, pathway enrichment, and gene-gene network analyses. The results showed that a total of 3760 genes were significantly differentially expressed and were categorized into cell adhesion molecules, cell junction proteins, chaperone, calcium-binding proteins, and membrane traffic proteins. Functional pathway analyses revealed that the TGF-β pathway, pentose phosphate pathway, and cell adhesion pathway play pivotal roles in the blood-retina barrier (BRB) and antioxidant defense system. Collectively, the data provide new insights into the molecular mechanisms of PlGF's biological functions in HRECs relevant to DR and diabetic macular edema (DME). The newly identified genes and

*Correspondence: huangh1@missouri.edu; Tel.: +1-573-882-9899 (H.H.).

Author Contributions Conceptualization, H.H. and M.S.S.; methodology, M.S.S. H.H., and L.F.; software, M.S.S..; formal analysis, M.S.; investigation, A.L. A.M, H.H., and M.S.S; resources, H.H.; data curation, H.H.; writing—original draft preparation, M.S.S., H.H., A.L., and A.M.; writing—review and editing, H.H., A.L., and A.M.; visualization, M.S.S., A.L and A.M.; supervision, H.H.; project administration, H.H.; funding acquisition, H.H.".

Availability of data and materials

All data generated and analyzed during this study are included in this published article and its supplementary information. RNA-Seq datasets were submitted to the NCBI-SRA (Sequence Read Archive (SRA) with accession numbers, SRA No: SRP239417; BioProject: PRJNA598727.

Conflicts of Interest

The authors have no conflict of interest to disclose in relation to this paper. The funders had no role in the design of the study; in the collection, analyses, or interpretation of data; in the writing of the manuscript; in the decision to publish the results.

pathways may act as disease markers and target molecules for therapeutic interventions for the patients with DR and DME refractory to the current anti-VEGF therapy.

Keywords

PlGF; RNA-seq; Gene ontology; KEGG; TGF-β; Diabetic Retinopathy

Introduction

Diabetic Retinopathy (DR) is the most common complication of diabetes and the leading cause of visual damage in the working-age adult population worldwide [1]. Increased glucose levels can lead to microvascular impairment in the retina. However, the mechanism by which hyperglycemia initiates retinal blood vessel damage in retinopathy remains intangible. It is well established that oxidative stress and inflammation play pivotal roles in the pathological process, consequently resulting in the breakdown of the blood-retinal barrier (BRB) [2]. An impaired BRB can further grow into augmented vascular retinal permeability and unbalanced growth of new blood vessels, thus prompting moderate to severe vision loss. When DR progresses into further advanced stages, vitreous hemorrhages can occur and result in retinal detachment and fibrovascular contraction, further advancing to vision loss, and eventually leading to blindness [3].

The identification of VEGF (vascular endothelial growth factor) as a crucial stimulus for proliferative diabetic retinopathy (PDR) and diabetic macular edema (DME) leads to the development of anti-VEGF therapies, which have improved the clinical management of these disease conditions. However, repeated anti-VEGF therapy in severe PDR and DME patients can lead to the formation of fibrovascular membranes (FVM) and tractional retinal detachment, which can cause severe vitreoretinal traction and hemorrhage [4]. Another study has also found that long-term intravitreal anti-VEGF injection may have detrimental effects on the neuronal cells, based on the survival and maintenance function of VEGF [5]. Thus, there is a clear need for alternative therapies for DR, especially for the non- or poor-responders to the current standard of care, with the potential to reduce the risk of treatment-related complications. Indeed, other crucial angiogenic growth factors are likely involved in this condition [6], which could serve as additional or even alternative targets for therapy. Cumulative evidence supports the pathogenic role of PlGF (placental growth factor), which is a member of the VEGF family and it was first identified from a human placental cDNA library in 1991 [7] [8]. PlGF is expressed in a number of cell types, including endothelial cells (ECs) and retinal pigment epithelial cells (RPEs) in response to hypoxia [9]. Like VEGF, PlGF can bind to fms-like tyrosine kinase-1 (FLT1), vascular endothelial growth factor receptor-1 (VEGFR-1), or its soluble isoform. The circulating isoform of sVEGFR-1 lacks the transmembrane and intracellular domains. The PlGF activates the FLT1 that affects the VEGF-VEGFR2 signaling, suggesting synergistic interactions of PlGF and VEGF. It can also bind to VEGF and form heterodimers [10] and employs a strong effect on blood vessel maturation and growth. Also, PlGF has direct proangiogenic effects on ECs [11]. Previously, we described that deleting PlGF in mice leads to reduced expression of diabetes-activated hypoxia-inducible factor (HIF)1α in the retina. We also found changes in the VEGF

pathway as well as expressions of VEGF, VEGFR1–3, HIF1α, and levels of phospho (p)–endothelial NOS (nitric oxide synthase), (p)-VEGFR1, and p-VEGFR2 in the retinas of diabetic PlGF knockout mice [12].

Despite the advances made, the biological function of PlGF and associated mechanisms are less well understood than those of its homolog VEGF. To bridge this gap, we sought to investigate the roles of PlGF in the EC barrier function and to elucidate the underlying molecular mechanisms. In one of the most recently completed studies [13], we found that PlGF inhibition promotes human retinal endothelial cell (HREC)'s barrier function, as indicated by increased resistance, upregulated expression levels of tight and adherens junction proteins, and their reinforced cell membrane localization. PlGF inhibition also prevents HREC's barrier dysfunction caused by high glucose, indicative of implication in DR. Additionally, we found that PlGF inhibition improves EC barrier function through activation of glucose-6-phosphate dehydrogenase (G6PD) and pentose phosphate pathway (PPP), as well as upregulation of antioxidant proteins.

In the present study, we identified transcriptome and pathways that are regulated by PlGF using the comparative transcriptomic analysis between the PlGF antibody (ab) treatment and the phosphate-buffered saline (PBS) control in the primary HREC. We provide a thorough report about the differentially expressed genes (DEGs) in HREC with the presence and absence of PlGF signaling and highlight several signaling pathways regulated by PlGF. Notably, the expression levels of many genes involved in the TGF-β signaling pathway, which acts as a primary regulator of many other identified genes and pathways, are altered in the PlGF ab treatment relative to the PBS control.

Materials and Methods

Primary human retinal endothelial cells (HRECs) culture

Primary HRECs were bought from Cell Systems (Cat#: ACBR1 181, Kirkland, WA). HRECs were seeded on fibronectin-coated (10 μg/ml, overnight, 33016015, Gibco) plastic culture vessels and grown using the EBM2-MV medium (Cat#: cc-4176, Lonza, Walkersville, MD) supplemented with 10% fetal bovine serum (FBS) (Cat#: SH3039603HI, Fisher Scientific, Waltham, MA), 1% of penicillin/streptomycin (P/S), and EGM MV Singlequots growth supplement kit (Cat#: cc-4147, Lonza). Cells were used during passage 5 to 6.

Cell treatments

At 80% confluence, the culture media was replaced with fresh media containing mouse anti-PlGF antibody (PL5D11D4), (25 μg/ml), and HRECs were collected 48 hours after the start of the incubation. PBS treated cells were used as a negative control. The primary HERC cultures treated with the validated neutralizing PlGF antibody have bearing on diabetic retinopathy (DR) in terms of two aspects. First, primary HREC cultures form a mono cell layer with barrier function maintained by the tight junctions and adherin junctions, such as ZO-1, Claudin 5, Occludin-1, and VE-Cadherin. These characteristics are highly relevant to DR because they can be disrupted by hyperglycemia and their expression levels represent

whether retinas develop diabetic complications to some extent. Second, PlGF antibody treatment promotes HREC barrier function not only in normal glucose conditions but also in high glucose condition (25mM D-glucose); the HREC with this glucose concentration is widely accepted *in vitro* model to study DR [13].

RNA extraction

Forty-eight hours after treatment, the cells were washed with PBS, and total RNA was extracted using the Qiagen mini RNA preparation kit (Qiagen) according to the manufacturer's protocol. RNA concentration was determined using a NanoDrop spectrophotometer (Thermo Scientific). RNA quality was determined using the Agilent bioanalyzer 2100 (Agilent Technologies). The analysis showed clear, defined 28s and 18s rRNA peaks, an indication of high-quality RNA. RIN value ≥ 8 was set as the cut-off for sample inclusion for downstream processing for RNA sequencing analysis.

RNA sequencing

RNA samples (6 PBS controls vs. 6 PlGF ab treatment) were submitted to Novogene Leading Edge Genomic Services & Solutions, California, USA, for sample preparation and sequencing. The DNase-treated to samples initially and evaluated for total RNA quality using the Agilent 2100 Bioanalyzer, subsequently 2 rounds of polyadenylate positive (poly A+) selection and conversion to cDNA. The Illumina HiSeq 2500 using for RNA sequencing with the latest versions of sequencing reagents and flow cells, providing up to 300 GB of sequence data per flow cell. In addition to that, the TruSeq library generation kits were used, giving to the manufacturer's instructions (Illumina) [14]. Library construction comprised of random fragmentation of the poly A+ mRNA, then cDNA production using random primers. The ends of the cDNA were repaired, adaptors and A-tailed ligated for indexing (up to 12 different barcodes per lane) in the sequencing run. The cDNA libraries were quantitated using qPCR in a Roche LightCycler 480 with the Kapa Biosystems kit for library quantitation (Kapa Biosystems) before cluster generation. Clusters were created to produce approximately 725K–825K clusters/mm2. Cluster quality and density were determined during the run after the first base addition parameters were measured. Paired-end 2 × 50 bp (basepair) sequencing runs were done to align the cDNA sequences to the reference human genome. Almost 15 million paired 50 bp reads were obtained per sample.

RNA-Seq bioinformatics analysis

The raw data were used for visualization of reads quality before and after pre-processing using FastQC software: (https://www.bioinformatics.babraham.ac.uk/projects/fastqc/) [15]. Then, the reads were processed to remove adapters, and ambiguous quality reads using the Trimmomatic-0.36 tool [16] [17] with trimming of bases from 3′ and 5′ end, maintaining the Phred-score ≤ 30. The human genome was downloaded from the National Centre for Biotechnology Information (NCBI) genome (https://www.ncbi.nlm.nih.gov/genome/?term=human) for reference-based assembly. We mapped all the datasets onto the human genome reference sequence GRCh38 using TopHat2.0.9 (http://ccb.jhu.edu/software/tophat/index.shtml). The expression levels were transformed into fragments per kilobase of exon per million mapped fragments (FPKM). We identified DEGs that satisfy the significance expressed as *q*-value representing FDR-adjusted *P* value < 0.05 by using Cufflinks 2.1.1

(http://cufflinks.cbcb.umd.edu). The Bioconductor tool with the CummeRbund package was employed to analyze differential expression analysis in the assembled transcriptome (http://compbio.mit.edu/cummeRbund/manual_2_0.html). Finally, both control and PlGF ab treated comparison transcript counts (matrix file) were used for differential gene expression using the CummeRbund package of Bioconductor with primary parameters such as FDR (false discovery rate), logFC (log fold-change), logCPM (log counts per million), and p-value. Unigenes with adjusted q-values of less than 0.05 ($p<0.05$) and the fold change of more than 2 ($logFC>2$) were considered as significantly differentially expressed genes.

Functional annotation

Gene ontology (GO) Enrichment Analysis (http://geneontology.org/page/go-enrichment-analysis) and DAVID annotation (https://david.ncifcrf.gov/) were used for functional annotation and pathways analysis. An adjusted EASE (Expression Analysis Systemic Explore Score) score of 0.05 and a threshold count of >2 genes were employed. Benjamin–Hochberg multiple testing correction was applied to the p-values. GO terms with FDR $q<0.05$ were considered significantly enriched within the gene set [16, 18].

Gene-gene network analysis

We performed the protein-protein network analysis for all DEGs using the STRING 10.5 database (https://string-db.org/). This is calculated in a variety of classification systems (Gene Ontology, KEGG, Pfam, and InterPro), and used the Fisher's exact test followed by a correction for multiple testing [19].

Statistical analysis

All numeric values were expressed as the mean ± standard deviation (SD) for the respective groups. Statistical analyses were performed using the cummeRbund R-package (https://www.bioconductor.org/packages/release/bioc/html/cummeRbund.html). Fisher's exact test and Benjamin–Hochberg corrections (FDR) were also used in the analyses of the two group comparisons. A p-value of less than 0.05 was considered significant.

Results

RNA sequencing

The cuffdiff results file was statistically analyzed and visualized using the cummeRbund package. The quality of the model fitting dispersion plot (Fig. 1A) showed the highest number of differentially expressed genes (DEGs). In addition, we calculated the distributions of FPKM (Fragments Per Kilobase of transcript per Million) scores across samples using the Density (Fig. 1B) plot and Box plot (Fig. 1C) respectively. We are visualized the coding sequence length (bp) (Fig. 1D), transcript length (bp) (Fig. 1E), genome span (bp) (Fig. 1F), 5' UTR length(bp) (Fig. 1G), 3' UTR length(bp) (Fig. 1H), and percentage of the GC content(Fig. 1I) of DEGs were predicted. In addition, the distribution of DEGs was predicted based on the human chromosomes, distribution of gene type, the number of exons (coding genes), and the number of transcript isoforms per coding gene (Fig. 2). We identified 53808 significant transcripts in total from the datasets. Among them, a total of 3760 differentially expressed genes (1750 up-regulated and 2010 down-regulated genes) that satisfy *q*-value

(FDR-corrected p-value) < 0.05 and fold change ≥ ±2.0, were identified in the PlGF ab treated group relative to the control. A hierarchical clustering heatmap (Fig. 3) and a volcano plot (Fig. 3A, Huang et al., 2019 [13]) are generated to represent the up- and down-regulated genes. These DEGs were used for further gene ontology and functional pathway analysis.

Functional annotation

DEGs were used for GO enrichment analysis using the DAVID annotation tool [20] with the complete human genome as the background. The following GO terms were enriched: molecular function (MF), biological process (BP), cellular component (CC), and protein classes (PC). Most of the DEGs were found to be involved in several molecular functions, such as binding (GO:0005488), catalytic activity (GO:0003824), and translation regulator activity (GO:0045182), respectively (Fig. 4A). The DEGs were also involved in various cellular components, i.e., cell (GO:0005623), organelle (GO:0043226), and protein-containing complex (GO:0032991) respectively (Fig. 4B). The DEGs were also involved in various biological processes, i.e., biological regulation (GO:0065007), cellular processes (GO:0009987), and metabolic process (GO:0008152), respectively (Fig. 4C). Most of the DEGs are classified as nucleic acid binding (PC00171), hydrolase (PC00121), transcription factor (PC00218), and enzyme modulator (PC00095) (Fig. 4D) respectively.

The gene ontology results revealed that the 36.9% of the genes were involved in binding (GO:0005488), 37.1% of genes were involved in catalytic activity (GO:0003824), and 6.9% of genes were involved in transcription regulator activity (GO:0140110) of molecular functions. A total of 44.5% of genes participated in the cell (GO:0005623), 34.0% of genes participated in the organelle (GO:0043226), and 11.4% of genes participated in the protein-containing complex (GO:0032991) of cellular components. A total of 32.8% of the genes were involved in cellular processes (GO:0009987), 24.6% of genes were involved in the metabolic process (GO:0008152), 15.9% of genes were involved in biological regulation (GO:0065007) and 11.0% of genes were involved in localization (GO:0051179) of biological processes. Finally, 16.2% of genes belonged to nucleic acid binding (PC00171), 11.9% of genes belonged to hydrolase (PC00121), 11.2% of genes belonged to the transcription factor (PC00218), 10.0% of genes belonged to enzyme modulator (PC00095), 9.4% of genes belonged to transferase (PC00220), 5.5% of genes belonged to cytoskeletal protein (PC00085), and 5.0% of genes belonged to the transporter (PC00227) of protein classes.

The functional enrichment results revealed genes (Fig.3B, Huang et al., 2019 [13]) mainly involved in the pentose phosphate pathway (Table 1), TGFβ signaling pathway (Table 2), as well as cell adhesion and antioxidant genes that we have identified and tabulated (Table 3); these are all up-regulated in PlGF ab treated conditions compared with the control. These results suggested that most of the genes involved in the TGFβ signaling pathway might have a beneficial role in diabetic retinopathy.

Pathway-focused gene interaction network analysis

We performed the gene-gene network analysis of genes within each pathway using the STRING tool (https://string-db.org/). Based on functional enrichment analysis, here we

focused on gene-gene interaction network analysis on the genes identified to be involved in the pentose phosphate pathway, carbon metabolism pathway, p53 signaling pathway, apoptosis pathway, pyrimidine metabolism pathway, ubiquitin-mediated proteolysis pathway, TGF-β pathway, and glycolysis pathways respectively.

The pentose phosphate pathway has 11 nodes, 33 edges, 6 average node degree, 0.842 avg. the local clustering coefficient, and 9 expected number of edges with a PPI enrichment p-value < 1.0e-16 (Suppl. Fig. 1A). The carbon metabolism pathway has 30 nodes, 195 edges, a 13 average node degree, 0.749 avg. the local clustering coefficient, and 9 expected number of edges with a PPI enrichment p-value < 1.0e-16 (Suppl. Fig. 1B). The p53 signaling pathway has 22 nodes, 111 edges, 10.1 average node degree, 0.75 avg. local clustering coefficient and 15 expected number of edges with a PPI enrichment p-value < 1.0e-16 (Suppl. Fig.1C). The apoptosis pathway has 31 nodes, 207 edges, a 13.4 average node degree, 0.728 avg. the local clustering coefficient, and 30 expected number of edges with a PPI enrichment p-value < 1.0e-16 (Suppl. Fig. 1D). The pyrimidine metabolism pathway has 27 nodes, 159 edges, 11.8 average node degree, 0.715 avg. the local clustering coefficient, and 12 expected number of edges with a PPI enrichment p-value < 1.0e-16 (Suppl. Fig. 2A). The ubiquitin-mediated proteolysis pathway has 15 nodes, 56 edges, a 7.47 average node degree, 0.717 avg. the local clustering coefficient, and 8 expected number of edges with a PPI enrichment p-value < 1.0e-16 (Suppl. Fig. 2B). The TGFβ signaling pathway has 37 nodes, 162 edges, an 8.76 average node degree, 0.606 avg. the local clustering coefficient, and 47 expected number of edges with a PPI enrichment p-value < 1.0e-16 (Suppl. Fig. 2C). The glycolysis pathway has 6 nodes, 15 edges, a 5.0 average node degree, 1 avg. the local clustering coefficient, and 1 expected number of edges with a PPI enrichment p-value < 1.0e-16 (Suppl. Fig. 2D). The results revealed that all pathway genes interact with each other directly or indirectly, except the EIF2S1 gene in the apoptosis pathway.

Gene-interaction network analysis of genes within the pentose phosphate pathway

Given our previous observation about the effect of PIGF on glucose-6-phosphate dehydrogenase (G6PD) and the antioxidant system [13], here we focused our analysis on the genes identified in the pentose phosphate pathway. Evidenced-based analysis of the genes showed that all the genes were inter-connected, and ALDOC was the query protein and first shell of interactors. Interestingly, G6PD, a gene that we previously found to be modulated under high glucose and by PlGF, was shown to interact with many genes such as PFKM, ALDOA, RPE, PGLS, and ALDOC (Suppl. Fig. 3A). An interaction analysis based on molecular action was also performed to gain insights into how these genes affect each other, and the results reveal that G6PD binds directly with PRPS1, PGLS, GPI, ALDOA, and ALDOC (Suppl. Fig. 3B). Based on confidence analysis, G6PD showed the highest interaction with GPI, RPE, PGLS, ALDOA, ALDOC, and high interaction with PRPS (Suppl. Fig. 3C). Reactome pathway analysis revealed that glycolysis and TP53 regulate metabolic genes and are among the enriched pathways, with FDR of 1.30e-09 and 0.0023, respectively. In addition, G6PD was involved in three of the 6 enriched Reactome pathways. The clustering of the 11 genes involved in the pentose phosphate pathway revealed two distinctive clusters. In one cluster, genes, G6PD, PGLS, RPE, and GP1 were grouped, while

PFKL, PFKM, ALDOC, ALDOA, DERA, and GLYCTK clustered together. PRPS1 was the only gene that did not cluster with any of the above (Suppl. Fig. 3D).

Gene-interaction network analysis of genes within the TGF-β signaling pathway

TGF-β signaling has been implicated in the pathophysiology of DR, for instance during the thickening of the capillary basal lamina, mediated via pericytes. Here, we performed an in-depth analysis of the genes identified from the pathway analysis involved in TGF-β signaling to understand how these genes interact with each other in modulating cell behavior after antibody-mediated inhibition of PlGF *in vitro*. The evidence-based analysis identified integrin beta-3 (ITGB4) as the query protein and the first shell of interactors (Fig. 5A), a protein thought to play a role in the hemidesmosome of epithelial cells. Analysis based on molecular function revealed that ITGB4 binds directly to PTK2, MET, ITGB3, CAV1, and SHC1, which in turn inhibit ZEB1 (Fig. 5B), and a confidence-based interaction analysis revealed that ITGB4 binds strongly with the above proteins (Fig. 6A). Cluster analysis of all the genes involved in the TGF-β pathway revealed three distinctive clusters of genes; Cluster 1 (green), cluster 2 (red), and cluster 3 (Dark cyan) (Fig. 6B). The volcano plot showed fold change and p-value of all TGFβ signaling pathway genes. The green color indicates down-regulated genes and the red color indicates up-regulated genes (Fig. 7).

The evidence-based analysis reveals that the ITGB4 binds directly to PTK2, MET, ITGB3, CAV1, and SHC1 genes, which in turn inhibit E-box-binding homeobox1 (ZEB1) in upstream condition but gene expression analysis results showed the PTK2, MET, ITGB3, CAV1, and SHC1 genes are down-regulated. It means the PTK2, MET, ITGB3, CAV1, and SHC1 genes are negatively up-regulate the ZEB1 gene. Overall, our results indicate that the ZEB1 gene may activate the transforming growth factor-β (TGFβ) signaling pathway.

Discussion

To reveal functional and molecular events in HREC with the presence and the absence of PlGF signaling, we performed a global transcriptome analysis to identify DEGs and functional enrichment analysis based on Illumina HiSeq2500 sequencing. To our knowledge, this is the first transcriptome-wide analysis to uncover DEGs that are expressed in presence and the absence of PlGF signaling. We anticipate that these data will be a powerful resource for future investigations into the effects of PlGF signaling responses in HREC cells.

The DEGs identified in the PIGF ab treated group relative to the control were further characterized and annotated by gene ontology and functional enrichment analysis. The downstream genes and pathways regulated by PlGF are potentially involved in the biological functions of PlGF, such as angiogenesis and EC barrier function.

One interesting class of genes are those involved in the pentose phosphate pathway and TGFβ signaling pathway. Our previous studies [13] [21] already disclosed the many attractive candidates of PPP pathway and their role in the activation of the antioxidant defense system in DR. The focus of the present study is TGFβ signaling pathway genes and their role in the activation of the antioxidant defense system in DR. The functional enrichment results revealed that the AKT1, APP, CAV1, CCND1, CDKN1A, DAB2, ETS1,

FN1, HDAC1, ITGB3, ITGB4, KLF11, LIMK2, MAPK9, MEF2C, MET, NEDD9, PML, PRKAR2A, PTK2, RAF1, ROCK1, SHC1, SMAD2, SMAD4, SNW1, SOS1, SPTBN1, STRAP, TGFB1I1, TGFBR3, TRAP1, UCHL5, WWP1, YAP1, ZEB1, and ZEB2 genes are involved in the TGFβ signaling pathway. TGFβ1 is a signaling protein involved in many processes, including immune system modulation, cell proliferation, cell differentiation, and apoptosis [22]. After activation, TGF-β binds to the type 2 TGF-β receptor, and this interaction leads to recruitment and subsequential phosphorylation of type 1 TGF-β receptor. In turn, the intracellular proteins Smad2 and Smad3 are recruited, and after forming a complex with Smad4, TGF-β translocates into the nucleus, where it activates downstream gene transcription [23].

There is evidence supporting that TGF-β1 can directly affect endothelial cell permeability such as in the blood-brain barrier (BBB) and BRB. Behzadian et al., (2001) [24] reported that TGF-β1 increases the retinal endothelial cell permeability by activation of MMP9 expression. Our results reveal that the MMP14 gene is up-regulated, which is in agreement with the observations by other investigators. A previous study reported that TGF-β1 signaling is complicated with autocrine and paracrine signaling conveyed by and for multiple cell types and with extensive detection of various receptor and ligand expressions [25]. Similarly, recent studies demonstrated that TGF-β1 signaling is required for both axon formation and migration [26]. The experimental results by Brionne et al. (2003) [27] showed that neural degeneration occurs in the brain of the TGF-β1 knockout mice. TGF-β1 is a multifunctional growth factor that is a well-established modulator of vascular cell integrity and function [28]. TGF-β1 is activated when endothelial and mesenchymal cell contact, and it is involved in the inhibition of EC proliferation and migration, vessel maturation, production of basement membranes, and induction of pericyte differentiation [29]. Pericytes and astrocytes may also release TGF-β1, which contributes to BBB/BRB integrity and function [30]. Recent studies have demonstrated that contact between endothelium cells (ECs) and pericytes or astrocytes leads to TGF-β1 activation (up-regulated), a major determinant of TGF-β1 availability and signaling [31]. Moreover, the loss of retinal pericytes has been speculated to be permissive for the progression of diabetic retinopathy [32]. These findings support the notion that the TGF-β1 signaling keeps the retinal microvascular integrity due to the high pericytes coverage. Our findings correlate well with the literature reports. Braunger et al. (2013) [33] described that the TGF-β1 signaling exerts several functions like the promotion of neuronal differentiation and the maintenance of neuronal survival in the retina. Shen et al. (2011) [34] demonstrated that TGF-β1 stimulus increases BBB permeability of both human brain ECs and bovine retinal ECs. The increased BBB permeability can be caused by tyrosine-phosphorylation of both VE-cadherin and claudin-5. TGF-β1signaling plays an essential role in the differentiation of vascular smooth muscle cells/pericytes at mid-gestation, as revealed by gene knockout studies on the signal components, such as Tgfbr2, TGF-β1, endoglin, Alk1, Alk5, Smad5, and Smad4 [35]. Our findings suggest that the SMAD2 and SMAD4 genes are down-regulated in the TGF-β1signaling pathway. This might have a significant role in dysregulation of the ubiquitin-proteasome pathway, angiogenesis pathway, p53 signaling pathway, and apoptosis pathway genes, as well as in up-regulation of the many cell-cell adhesion genes like LGALS3, FBN2, FBN1, LTBP4, GPNMB, CELSR1, ITGB4, TMEM8B, MFGE8, ITGB3, SDC1,

MAGED4B, MPZL1, ITGB2, CCBE1, and MAGED2, and increase of the BBB permeability.

The other genes of interest from the pentose phosphate pathway and antioxidant defense system, the glycolysis, and carbon metabolism genes, play a beneficial role in diabetes-related oxidative damage to retinal cells (diabetic retinopathy). Oxidative stress is triggered by an imbalance between the production of reactive oxygen species (ROS) and the loss of antioxidant defense components [36] [37]. G6PD gene plays a key role in regulating carbon flow through the pentose phosphate pathway. Specifically, the enzyme affects the production of the reduced form of the extramitochondrial nicotine adenosine dinucleotide phosphate (NADPH) coenzyme by controlling the conversion from glucose-6-phosphate to 6-phosphogluconate in the pentose phosphate pathway. In red blood cells, defense against oxidative damage is heavily dependent on G6PD activity, which is the only source of NADPH [38] [21]. Our outcomes propose that the G6PD gene is up-regulated in the PlGF ab treated condition. It stimulates the oxidative branch of PPP to supply cytosolic NADPH to counteract oxidative damage as well as up-regulating antioxidant genes such as Peroxiredoxin (Prdx)1, Prdx3, and Prdx6. Prdxs are highly conserved and small molecular weight (20–30 kDa) thiol peroxidases that scavenge alkyl hydroperoxides, hydrogen peroxide (H_2O_2), and peroxynitrite inactive cells [39]. Prdxs play a pivotal role in the protection of cells from oxidative stress. Furthermore, cumulative evidence supports that Prdxs can also perform as redox sensors in the condition of oxidative stress and the local accumulation of hydrogen peroxide [40]. In the retina, after expressing of Prdx6, the Müller cells and astrocytes display central roles in the maintenance of the BRB (blood-retinal barrier) function. Moreover, several studies found that the blood-retinal barrier is compromised due to decreased Prdx6 in several disease conditions like diabetic retinopathy (DR), age-related macular degeneration (AMD), arterial and venous occlusions [16] [39] [41]. Our previous proteomics studies also reported that PlGF absence increases neuroprotective and antioxidant proteins in the diabetic mouse retina such as Prdx6 and Map2 [16]. Recent studies on tears from patients with glaucoma have also identified Prdx1 as having possible involvement in inflammation [42]. Furthermore, apart from their role as antioxidants, the peroxiredoxins can affect a diverse range of biological processes that include cellular proliferation, differentiation, and apoptosis by influencing signal transduction pathways that employ hydrogen peroxide as a secondary messenger [43]. The above reports relavant to our results and suggest that Prdx1, Prdx3, and Prdx6 play a role in defending oxidative stress in DR. Based on all together, the relevance and possible regulatory role of TGFβ pathway DEGs increased BBB permeability. However, further work must be perform to verify the function and relationship between TGFβ signaling and antioxidant defence process in BBB permeability.

Limitations of the study

1. The present study only presented the transcriptome and pathway differences between HREC cultures treated with PlGF antibody and the cultures with the presence of PlGF signaling. Although some of the differentially expressed genes, such as G6PD, PRDX3, PRD6, and VECadherin, were validated on the mRNA and/or protein levels and reported in our publications [13] [21], additional

validation results of RNA seq and bioinformatics results would corroborate our conclusions, particularly for those TGF-β pathway genes.

2. HREC cultures were used for experimental models to investigate the molecular pathways modulated by PlGF signaling and relevant to diabetic retinopathy. Although primary HREC culture is a widely accepted *in vitro* model, some more physiologically relevant model, such as vascular organoids and transgenic mice, would be used for further study on the function of the candidate genes identified through RNA seq and bioinformatics analyses.

3. We used the PlGF neutralizing antibody (PL5D11D4), which was developed to block mouse PlGF signaling through the interaction with VEGFR1 [44]. Characterization of this antibody and effects on cancer and eye disease have been performed in both rodent and human models [45]. We validated that this antibody can bind with human PlGF and also observed the clear biological effects on HREC integrity and function1. Despite these characterizations, whether this antibody can interfere with the interaction of human PlGF and VEGFR1 and what concentrations can effectively block its downstream signaling are to be defined.

4. The effects of PlGF on HREC barrier function are explicit, however, it is unclear why and how the neutralizing antibody to PIGF would be expected to have effects on the HREC. Given PlGF is expressed by HREC and can be regulated by VEGF [46], it is most likely that PlGF acts on HREC in an autocrine fashion.

Conclusion

Our results demonstrated that neutralizing PlGF regulates a variety of gene expressions that are relevant to its pathophysiological functional roles, such as angiogenesis and EC barrier function. Among the most important ones are those genes involved in TGFβ, PPP, and the antioxidant defense system. These newly identified genes and pathways may act as potential target molecules for therapeutic interventions for those patients with DR refractory to the current anti-VEGF therapy.

Supplementary Material

Refer to Web version on PubMed Central for supplementary material.

Acknowledgments

The authors wish to acknowledge the contribution of the Division of Information Technology (UM system) University of Missouri (Columbia, MO, USA) for High-Performance Computing (HPC) facilities and Mr. Dmitry Rumyancev (Belgorod, Russia) for the graphical abstract artwork assets. The early version of the manuscript was deposited to www.preprints.org (https://www.preprints.org/manuscript/201907.0140/v1) under the title “Pathway-Focused Gene Interaction Analysis Reveals the Regulation of TGFβ, Pentose Phosphate and Antioxidant Defense System by Placental Growth Factor in Retinal Endothelial Cell Functions: Implication in Diabetic Retinopathy.” And was assigned DOI 10.20944/preprints201907.0140.v1.

Funding

This work was supported by MU start-up funds and NIH grant (EY027824 to H.H.).

References

1. Lee R, Wong TY and Sabanayagam C (2015) Epidemiology of diabetic retinopathy, diabetic macular edema and related vision loss. Eye Vis (Lond) 2:17. doi: 10.1186/s40662-015-0026-2 [PubMed: 26605370]
2. Curtis TM, Gardiner TA and Stitt AW (2009) Microvascular lesions of diabetic retinopathy: clues towards understanding pathogenesis? Eye (Lond) 23:1496–508. doi: 10.1038/eye.2009.108 [PubMed: 19444297]
3. Friedlander M (2007) Fibrosis and diseases of the eye. J Clin Invest 117:576–86. doi: 10.1172/JCI31030 [PubMed: 17332885]
4. Diabetic Retinopathy Clinical Research N, Elman MJ, Aiello LP, Beck RW, Bressler NM, Bressler SB, Edwards AR, Ferris FL 3rd, Friedman SM, Glassman AR, Miller KM, Scott IU, Stockdale CR and Sun JK (2010) Randomized trial evaluating ranibizumab plus prompt or deferred laser or triamcinolone plus prompt laser for diabetic macular edema. Ophthalmology 117:1064–1077 e35. doi: 10.1016/j.ophtha.2010.02.031 [PubMed: 20427088]
5. Storkebaum E and Carmeliet P (2004) VEGF: a critical player in neurodegeneration. J Clin Invest 113:14–8. doi: 10.1172/JCI20682 [PubMed: 14702101]
6. Aiello LP (2005) Angiogenic pathways in diabetic retinopathy. N Engl J Med 353:839–41. doi: 10.1056/NEJMe058142 [PubMed: 16120866]
7. Maglione D, Guerriero V, Viglietto G, Delli-Bovi P and Persico MG (1991) Isolation of a human placenta cDNA coding for a protein related to the vascular permeability factor. Proc Natl Acad Sci U S A 88:9267–71. [PubMed: 1924389]
8. Saddala MS, Lennikov A, Grab DJ, Liu GS, Tang S and Huang H (2018) Proteomics reveals ablation of PlGF increases antioxidant and neuroprotective proteins in the diabetic mouse retina. Sci Rep 8:16728. doi: 10.1038/s41598-018-34955-x [PubMed: 30425286]
9. Ohno-Matsui K, Uetama T, Yoshida T, Hayano M, Itoh T, Morita I and Mochizuki M (2003) Reduced retinal angiogenesis in MMP-2-deficient mice. Invest Ophthalmol Vis Sci 44:5370–5. doi: 10.1167/iovs.03-0249 [PubMed: 14638740]
10. Autiero M, Waltenberger J, Communi D, Kranz A, Moons L, Lambrechts D, Kroll J, Plaisance S, De Mol M, Bono F, Kliche S, Fellbrich G, Ballmer-Hofer K, Maglione D, Mayr-Beyrle U, Dewerchin M, Dombrowski S, Stanimirovic D, Van Hummelen P, Dehio C, Hicklin DJ, Persico G, Herbert JM, Communi D, Shibuya M, Collen D, Conway EM and Carmeliet P (2003) Role of PlGF in the intra- and intermolecular cross talk between the VEGF receptors Flt1 and Flk1. Nat Med 9:936–43. doi: 10.1038/nm884 [PubMed: 12796773]
11. Carmeliet P, Moons L, Luttun A, Vincenti V, Compernolle V, De Mol M, Wu Y, Bono F, Devy L, Beck H, Scholz D, Acker T, DiPalma T, Dewerchin M, Noel A, Stalmans I, Barra A, Blacher S, VandenDriessche T, Ponten A, Eriksson U, Plate KH, Foidart JM, Schaper W, Charnock-Jones DS, Hicklin DJ, Herbert JM, Collen D and Persico MG (2001) Synergism between vascular endothelial growth factor and placental growth factor contributes to angiogenesis and plasma extravasation in pathological conditions. Nat Med 7:575–83. doi: 10.1038/87904 [PubMed: 11329059]
12. Huang H, He J, Johnson D, Wei Y, Liu Y, Wang S, Lutty GA, Duh EJ and Semba RD (2015) Deletion of placental growth factor prevents diabetic retinopathy and is associated with Akt activation and HIF1alpha-VEGF pathway inhibition. diabetes 2015;64:200–212. Diabetes 64:1067. doi: 10.2337/db15-er03
13. Huang H, Lennikov A, Saddala MS, Gozal D, Grab DJ, Khalyfa A and Fan L (2019) Placental growth factor negatively regulates retinal endothelial cell barrier function through suppression of glucose-6-phosphate dehydrogenase and antioxidant defense systems. FASEB J 33:13695–13709. doi: 10.1096/fj.201901353R [PubMed: 31585507]
14. Saddala MS, Lennikov A, Mukwaya A and Huang H (2020) Transcriptome-Wide Analysis of CXCR5 Deficient Retinal Pigment Epithelial (RPE) Cells Reveals Molecular Signatures of RPE Homeostasis. Biomedicines 8. doi: 10.3390/biomedicines8060147
15. annotation Saddala MS, Lennikov A, Bouras A and Huang H (2020) RNA-Seq reveals differential expression profiles and functional of genes involved in retinal degeneration in Pde6c mutant Danio rerio. BMC Genomics 21:132. doi: 10.1186/s12864-020-6550-z [PubMed: 32033529]

16. Saddala MS, Lennikov A, Mukwaya A, Fan L, Hu Z and Huang H (2019) Transcriptome-wide analysis of differentially expressed chemokine receptors, SNPs, and SSRs in the age-related macular degeneration. Hum Genomics 13:15. doi: 10.1186/s40246-019-0199-1 [PubMed: 30894217]
17. Bolger AM, Lohse M and Usadel B (2014) Trimmomatic: a flexible trimmer for Illumina sequence data. Bioinformatics 30:2114–20. doi: 10.1093/bioinformatics/btu170 [PubMed: 24695404]
18. Huang DW, Sherman BT, Tan Q, Kir J, Liu D, Bryant D, Guo Y, Stephens R, Baseler MW, Lane HC and Lempicki RA (2007) DAVID Bioinformatics Resources: expanded annotation database and novel algorithms to better extract biology from large gene lists. Nucleic Acids Res 35:W169–75. doi: 10.1093/nar/gkm415 [PubMed: 17576678]
19. Rivals I, Personnaz L, Taing L and Potier MC (2007) Enrichment or depletion of a GO category within a class of genes: which test? Bioinformatics 23:401–7. doi: 10.1093/bioinformatics/btl633 [PubMed: 17182697]
20. Dennis G Jr., Sherman BT, Hosack DA, Yang J, Gao W, Lane HC and Lempicki RA (2003) DAVID: Database for Annotation, Visualization, and Integrated Discovery. Genome Biol 4:P3. [PubMed: 12734009]
21. Saddala MS, Lennikov A and Huang H (2020) Placental growth factor regulates the pentose phosphate pathway and antioxidant defense systems in human retinal endothelial cells. J Proteomics 217:103682. doi: 10.1016/j.jprot.2020.103682 [PubMed: 32058040]
22. Yoshimura A, Wakabayashi Y and Mori T (2010) Cellular and molecular basis for the regulation of inflammation by TGF-beta. J Biochem 147:781–92. doi: 10.1093/jb/mvq043 [PubMed: 20410014]
23. Derynck R and Zhang YE (2003) Smad-dependent and Smad-independent pathways in TGF-beta family signalling. Nature 425:577–84. doi: 10.1038/nature02006 [PubMed: 14534577]
24. Behzadian MA, Wang XL, Windsor LJ, Ghaly N and Caldwell RB (2001) TGF-beta increases retinal endothelial cell permeability by increasing MMP-9: possible role of glial cells in endothelial barrier function. Invest Ophthalmol Vis Sci 42:853–9. [PubMed: 11222550]
25. Close JL, Gumuscu B and Reh TA (2005) Retinal neurons regulate proliferation of postnatal progenitors and Muller glia in the rat retina via TGF beta signaling. Development 132:3015–26. doi: 10.1242/dev.01882 [PubMed: 15944186]
26. Yi JJ, Barnes AP, Hand R, Polleux F and Ehlers MD (2010) TGF-beta signaling specifies axons during brain development. Cell 142:144–57. doi: 10.1016/j.cell.2010.06.010 [PubMed: 20603020]
27. Brionne TC, Tesseur I, Masliah E and Wyss-Coray T (2003) Loss of TGF-beta 1 leads to increased neuronal cell death and microgliosis in mouse brain. Neuron 40:1133–45. doi: 10.1016/s0896-6273(03)00766-9 [PubMed: 14687548]
28. ten Dijke P and Arthur HM (2007) Extracellular control of TGFbeta signalling in vascular development and disease. Nat Rev Mol Cell Biol 8:857–69. doi: 10.1038/nrm2262 [PubMed: 17895899]
29. Neubauer K, Kruger M, Quondamatteo F, Knittel T, Saile B and Ramadori G (1999) Transforming growth factor-beta1 stimulates the synthesis of basement membrane proteins laminin, collagen type IV and entactin in rat liver sinusoidal endothelial cells. J Hepatol 31:692–702. doi: 10.1016/s0168-8278(99)80350-x [PubMed: 10551394]
30. Obermeier B, Daneman R and Ransohoff RM (2013) Development, maintenance and disruption of the blood-brain barrier. Nat Med 19:1584–96. doi: 10.1038/nm.3407 [PubMed: 24309662]
31. Song L, Yan Y, Marzano M and Li Y (2019) Studying Heterotypic Cell(−)Cell Interactions in the Human Brain Using Pluripotent Stem Cell Models for Neurodegeneration. Cells 8. doi: 10.3390/cells8040299
32. Hammes HP (2005) Pericytes and the pathogenesis of diabetic retinopathy. Horm Metab Res 37 Suppl 1:39–43. doi: 10.1055/s-2005-861361 [PubMed: 15918109]
33. Braunger BM, Pielmeier S, Demmer C, Landstorfer V, Kawall D, Abramov N, Leibinger M, Kleiter I, Fischer D, Jagle H and Tamm ER (2013) TGF-beta signaling protects retinal neurons from programmed cell death during the development of the mammalian eye. J Neurosci 33:14246–58. doi: 10.1523/JNEUROSCI.0991-13.2013 [PubMed: 23986258]
34. Shen W, Li S, Chung SH, Zhu L, Stayt J, Su T, Couraud PO, Romero IA, Weksler B and Gillies MC (2011) Tyrosine phosphorylation of VE-cadherin and claudin-5 is associated with TGF-beta1-

induced permeability of centrally derived vascular endothelium. Eur J Cell Biol 90:323–32. doi: 10.1016/j.ejcb.2010.10.013 [PubMed: 21168935]

35. Lan Y, Liu B, Yao H, Li F, Weng T, Yang G, Li W, Cheng X, Mao N and Yang X (2007) Essential role of endothelial Smad4 in vascular remodeling and integrity. Mol Cell Biol 27:7683–92. doi: 10.1128/MCB.00577-07 [PubMed: 17724086]
36. Masuda T, Shimazawa M and Hara H (2017) Retinal Diseases Associated with Oxidative Stress and the Effects of a Free Radical Scavenger (Edaravone). Oxid Med Cell Longev 2017:9208489. doi: 10.1155/2017/9208489 [PubMed: 28194256]
37. Saddala MS, Lennikov A and Huang H (2020) Discovery of Small-Molecule Activators for Glucose-6-Phosphate Dehydrogenase (G6PD) Using Machine Learning Approaches. Int J Mol Sci 21. doi: 10.3390/ijms21041523
38. Pinna A, Carru C, Solinas G, Zinellu A and Carta F (2007) Glucose-6-phosphate dehydrogenase deficiency in retinal vein occlusion. Invest Ophthalmol Vis Sci 48:2747–52. doi: 10.1167/iovs.06-1064 [PubMed: 17525208]
39. Chidlow G, Wood JP, Knoops B and Casson RJ (2016) Expression and distribution of peroxiredoxins in the retina and optic nerve. Brain Struct Funct 221:3903–3925. doi: 10.1007/s00429-015-1135-3 [PubMed: 26501408]
40. Rhee SG and Woo HA (2011) Multiple functions of peroxiredoxins: peroxidases, sensors and regulators of the intracellular messenger H(2)O(2), and protein chaperones. Antioxid Redox Signal 15:781–94. doi: 10.1089/ars.2010.3393 [PubMed: 20919930]
41. Cai J, Ahmad S, Jiang WG, Huang J, Kontos CD, Boulton M and Ahmed A (2003) Activation of vascular endothelial growth factor receptor-1 sustains angiogenesis and Bcl-2 expression via the phosphatidylinositol 3-kinase pathway in endothelial cells. Diabetes 52:2959–68. doi: 10.2337/diabetes.52.12.2959 [PubMed: 14633857]
42. Pieragostino D, Agnifili L, Fasanella V, D'Aguanno S, Mastropasqua R, Di Ilio C, Sacchetta P, Urbani A and Del Boccio P (2013) Shotgun proteomics reveals specific modulated protein patterns in tears of patients with primary open angle glaucoma naive to therapy. Mol Biosyst 9:1108–16. doi: 10.1039/c3mb25463a [PubMed: 23580065]
43. Immenschuh S and Baumgart-Vogt E (2005) Peroxiredoxins, oxidative stress, and cell proliferation. Antioxid Redox Signal 7:768–77. doi: 10.1089/ars.2005.7.768 [PubMed: 15890023]
44. Fischer C, Jonckx B, Mazzone M, Zacchigna S, Loges S, Pattarini L, Chorianopoulos E, Liesenborghs L, Koch M, De Mol M, Autiero M, Wyns S, Plaisance S, Moons L, van Rooijen N, Giacca M, Stassen JM, Dewerchin M, Collen D and Carmeliet P (2007) Anti-PlGF inhibits growth of VEGF(R)-inhibitor-resistant tumors without affecting healthy vessels. Cell 131:463–75. doi: 10.1016/j.cell.2007.08.038 [PubMed: 17981115]
45. Van de Veire S, Stalmans I, Heindryckx F, Oura H, Tijeras-Raballand A, Schmidt T, Loges S, Albrecht I, Jonckx B, Vinckier S, Van Steenkiste C, Tugues S, Rolny C, De Mol M, Dettori D, Hainaud P, Coenegrachts L, Contreres JO, Van Bergen T, Cuervo H, Xiao WH, Le Henaff C, Buysschaert I, Kharabi Masouleh B, Geerts A, Schomber T, Bonnin P, Lambert V, Haustraete J, Zacchigna S, Rakic JM, Jimenez W, Noel A, Giacca M, Colle I, Foidart JM, Tobelem G, Morales-Ruiz M, Vilar J, Maxwell P, Vinores SA, Carmeliet G, Dewerchin M, Claesson-Welsh L, Dupuy E, Van Vlierberghe H, Christofori G, Mazzone M, Detmar M, Collen D and Carmeliet P (2010) Further pharmacological and genetic evidence for the efficacy of PlGF inhibition in cancer and eye disease. Cell 141:178–90. doi: 10.1016/j.cell.2010.02.039 [PubMed: 20371353]
46. Yao YG, Yang HS, Cao Z, Danielsson J and Duh EJ (2005) Upregulation of placental growth factor by vascular endothelial growth factor via a post-transcriptional mechanism. FEBS Lett 579:1227–34. doi: 10.1016/j.febslet.2005.01.017 [PubMed: 15710418]

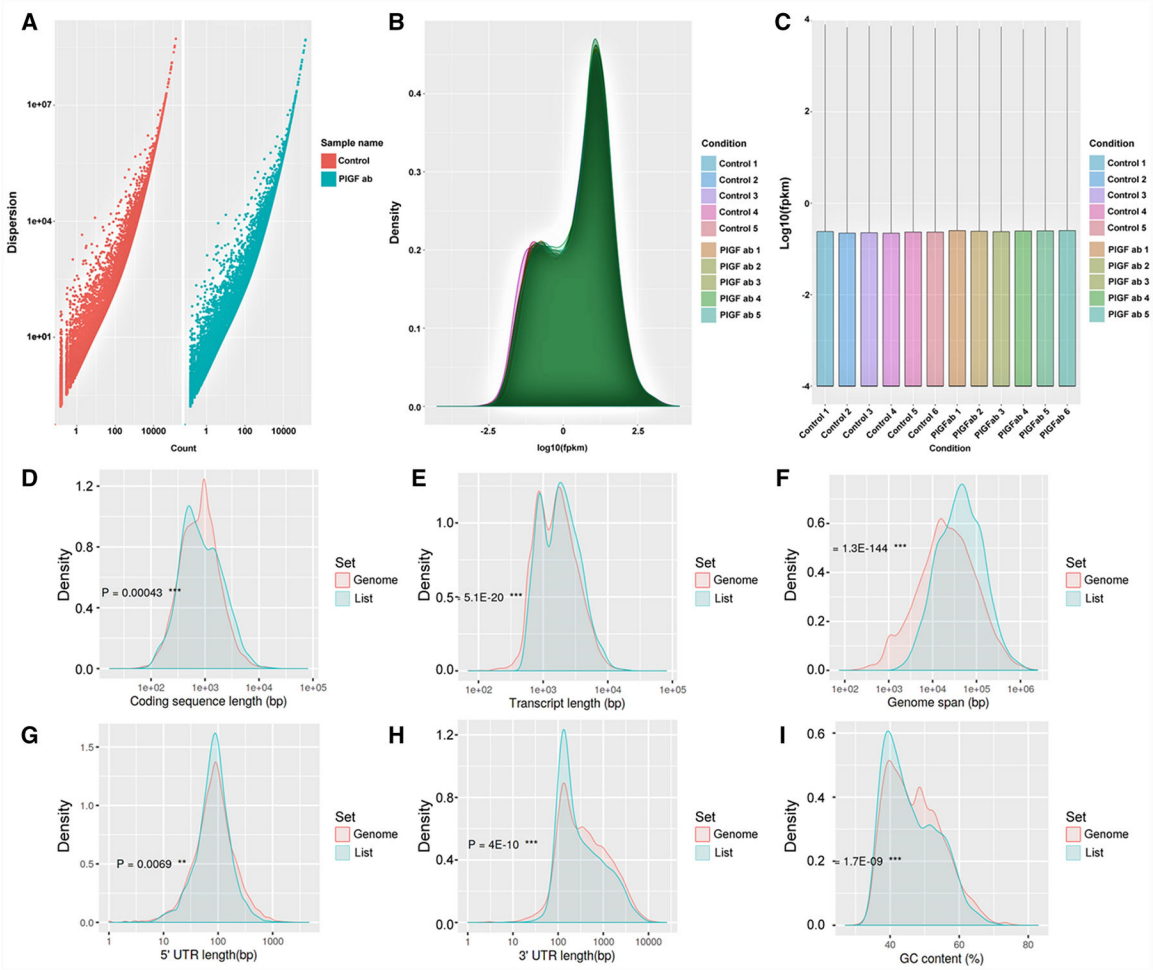

Figure 1.

The quality of a higher number of differentially expressed genes representation and raw sequencing component analysis on the reference genome A. Model fitting dispersion plot. B. Density plot C. Box plot. D. Coding sequence length(bp) E. Transcript length(bp) F. Genome span(bp), G. 5' UTR length(bp) H. 3' UTR length(bp) I. Percentage of GC content in DEGs.

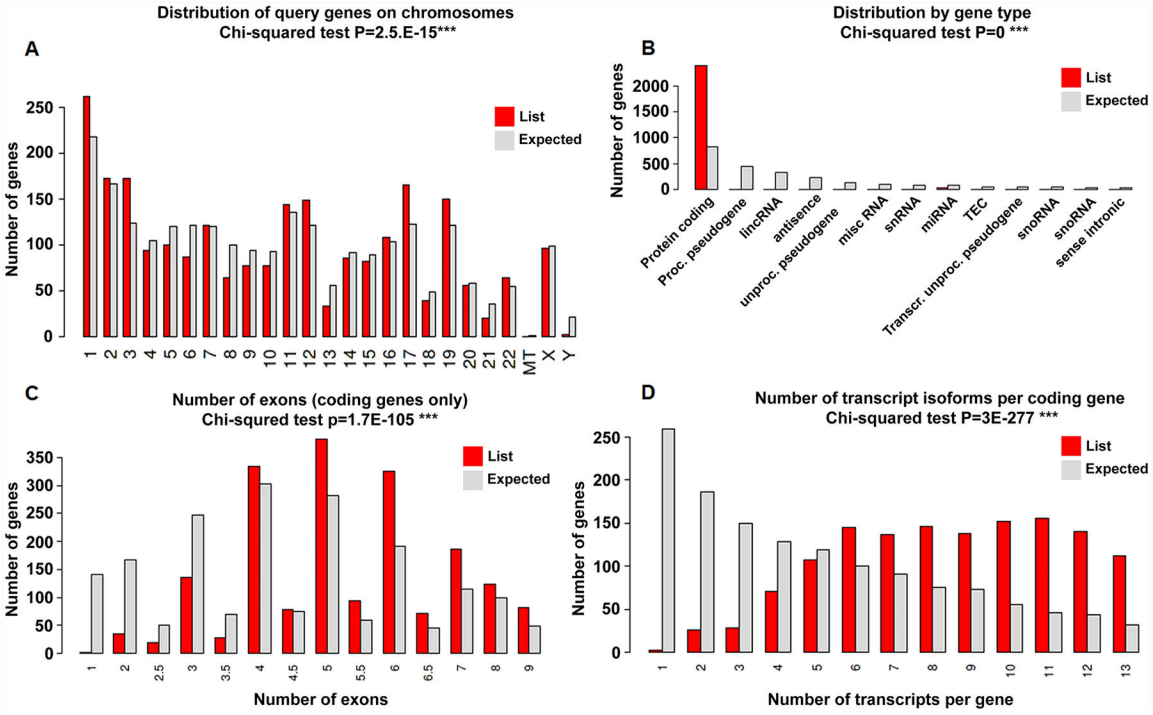

Figure 2.

Distribution of DEGs sequencing component analysis A. Distribution of DEGs chromosomes B. Distribution of gene type C. Number of exons (coding genes) D. Number of transcript isoforms per coding gene.

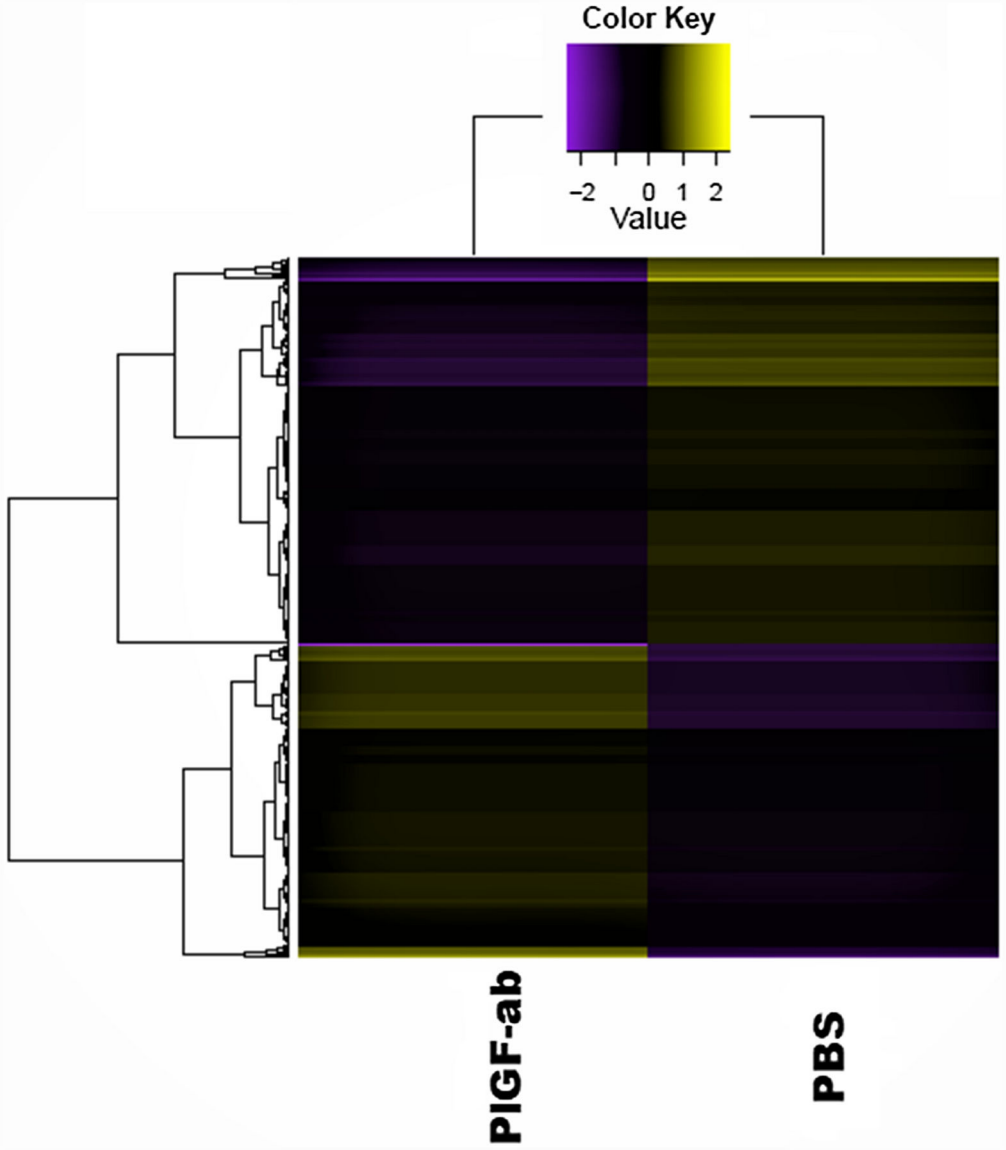

Figure 3.

Gene expression profile in PlGF ab treated group relative to the control. A. The differentially expressed genes are plotted in the form of a heat map, where red color represents down-regulated, while the green color represents up-regulated (logFC±2; p-values < 0.05). The dendrogram provides a hierarchical clustering. The FDR< 0.05, P-value <0.05 are considered as statistical significances.

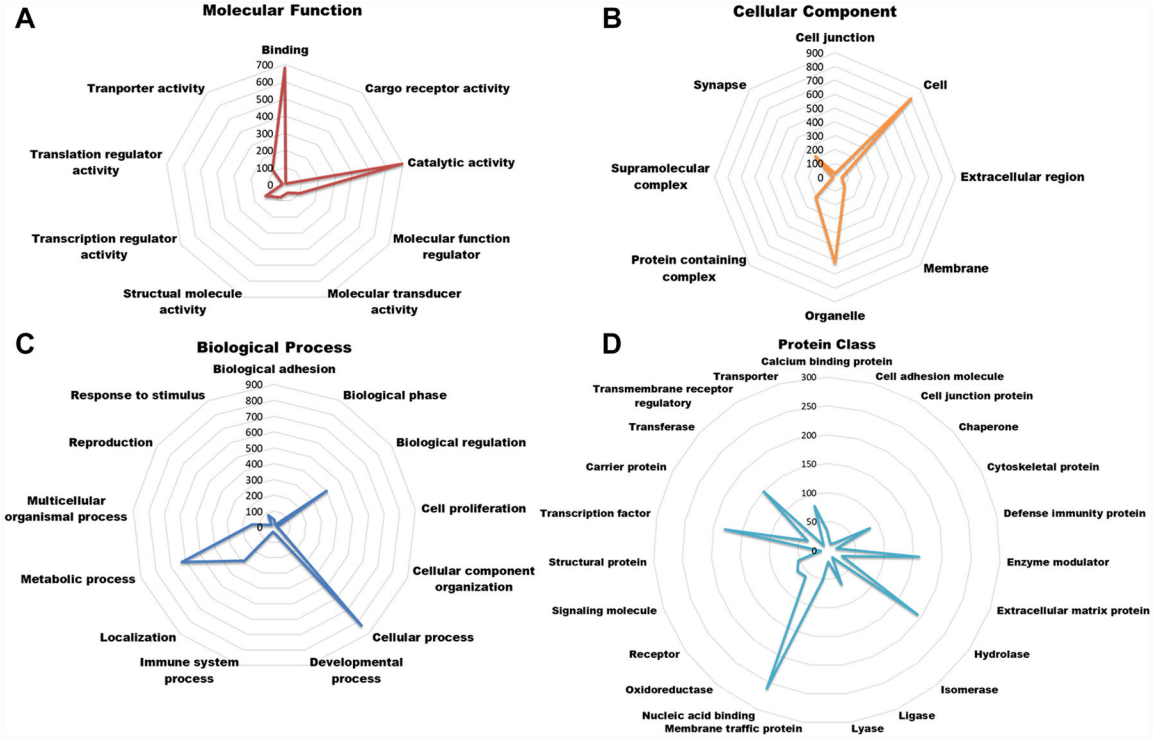

Figure 4.

Gene expression profile in the group treated with PlGF antibody relative to the control. A. Molecular function (MF) B. Cellular component (CC) C. Biological process (BP) D. Protein class of DEGs. The FDR< 0.05, P-value <0.05 are considered as statistical significances.

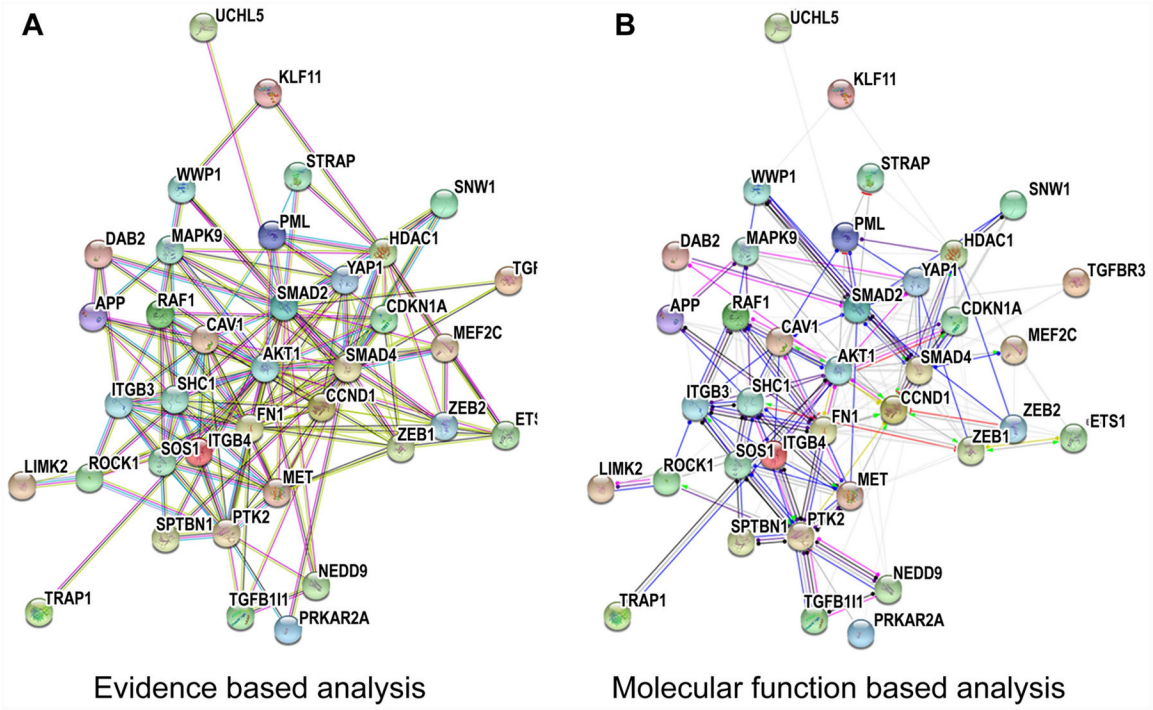

Figure 5.

Interaction network analysis of genes involved in the TGF-beta signaling pathway. A is the evidence-based interaction network analysis, B is the molecular function-based interaction network analysis. Each gene is represented as a different color sphere.

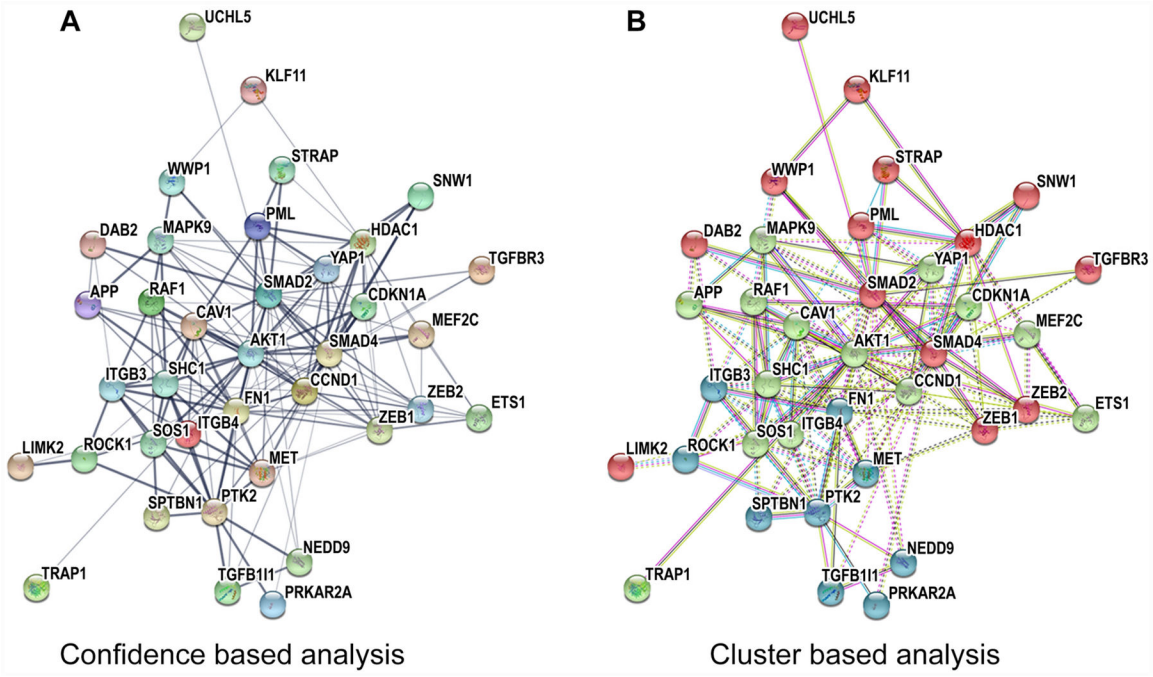

Figure 6.

Interaction network analysis of genes involved in the TGF-beta signaling pathway. A is the confidence-based interaction network analysis, and B is a k means cluster analysis of the genes. Each gene is represented as a different color sphere. k means cluster analysis of the genes divided into three clusters, cluster one represents red color, cluster two represents green color, and cluster three represents the blue color.

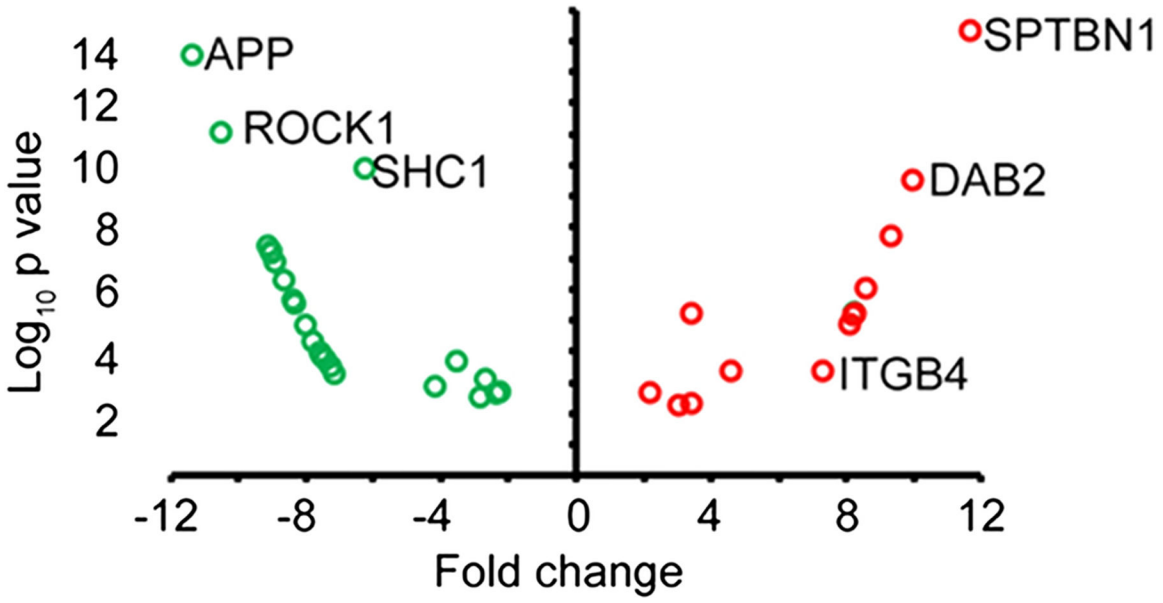

Figure 7.

The volcano plot showed fold change and p-value of all TGFβ signaling pathway genes. The green color indicates down-regulated genes and the red color indicates up-regulated genes.

Table 1.

List of Pentose phosphate pathway genes along with Ensembl, gene symbol, gene name logFC, p-values in RNA seq data analysis.

Pentose phosphate pathway				
Ensembl	**Gene Symbol**	**Gene Name**	**logFC**	**p-value**
ENST00000566012	ALDOA	aldolase, fructose-bisphosphate A	−2.70711	0.000159
ENST00000226253	ALDOC	aldolase, fructose-bisphosphate C	−8.29613	3.54E-06
ENST00000533447	DERA	deoxyribose-phosphate aldolase	3.07566	0.000305
ENSG00000160211	G6PD*	glucose-6-phosphate dehydrogenase	6.20824	1.08E-12
ENST00000486393	GLYCTK	glycerate kinase	−7.43140	0.000164
ENST00000588991	GPI	glucose-6-phosphate isomerase	−7.36468	0.000217
ENST00000397961	PFKL	phosphofructokinase, liver type	7.15971	0.000530
ENST00000551339	PFKM	phosphofructokinase, muscle	−10.6579	2.97E-12
ENST00000594761	PGLS	6-phosphogluconolactonase	7.41946	0.000217
ENST00000372419	PRPS1	phosphoribosyl pyrophosphate synthetase 1	−8.25372	4.28E-06
ENST00000429907	RPE	ribulose-5-phosphate-3-epimerase	7.75075	4.53E-05

*The protein change of G6PD was validated (Huang et al., 2019 and Saddala et al., 2020)[18, 39].

Table 2.

List of TGF-β pathway genes along with Ensembl, gene symbol, gene name logFC, p-values in RNA seq data analysis.

Ensembl	Gene Symbol	Gene Name	logFC	p-value
ENST00000544168	AKT1	AKT serine/threonine kinase 1	−2.365428775	0.0023003
ENST00000474136	APP	amyloid beta precursor protein	−11.37328742	2.77E-14
ENST00000393468	CAV1	caveolin 1	−2.252194366	0.00204467
ENST00000542367	CCND1	cyclin D1	3.391893687	5.44E-06
ENST00000405375	CDKN1A	cyclin dependent kinase inhibitor 1A	−8.013577331	1.45E-05
ENST00000509337	DAB2	DAB2, clathrin adaptor protein	9.945707367	2.78E-10
ENST00000526145	ETS1	ETS proto-oncogene 1, transcription factor	3.384794454	0.00455057
ENST00000474036	FN1	fibronectin 1	3.02069906	0.00472911
ENST00000428704	HDAC1	histone deacetylase 1	−7.143753011	0.00053040
ENST00000560629	ITGB3	integrin subunit beta 3	−7.614824773	9.64E-05
ENST00000200181	ITGB4	integrin subunit beta 4	7.294499935	0.00039082
ENST00000535335	KLF11	Kruppel like factor 11	8.042834182	1.17E-05
ENST00000333611	LIMK2	LIM domain kinase 2	8.171648208	6.32E-06
ENST00000393362	MAPK9	mitogen-activated protein kinase 9	−2.849607483	0.00291167
ENST00000504921	MEF2C	myocyte enhancer factor 2C	−8.39414907	2.05E-06
ENST00000318493	MET	MET proto-oncogene, receptor tyrosine kinase	−8.922971532	1.28E-07
ENST00000504387	NEDD9	neural precursor cell expressed, developmentally down-regulated 9	2.177612821	0.00196987
ENST00000567606	PML	promyelocytic leukemia	−9.040096253	5.90E-08
ENST00000296446	PRKAR2A	protein kinase cAMP-dependent type II regulatory subunit alpha	−8.667581639	4.66E-07
ENST00000521791	PTK2	protein tyrosine kinase 2	−4.161512038	0.00133434
ENST00000423275	RAF1	Raf-1 proto-oncogene, serine/threonine kinase	−9.032436585	6.69E-08
ENST00000635540	ROCK1	Rho associated coiled-coil containing protein kinase 1	−10.50374244	8.23E-12
ENST00000368453	SHC1	SHC adaptor protein 1	−6.232971845	1.30E-10
ENST00000402690	SMAD2	SMAD family member 2	−2.662985055	0.00074433
ENST00000398417	SMAD4	SMAD family member 4	−7.777534707	4.53E-05
ENST00000555761	SNW1	SNW domain containing 1	−7.431403503	0.00016479
ENST00000426016	SOS1	SOS Ras/Rac guanine nucleotide exchange factor 1	−8.32564549	2.94E-06
ENST00000389980	SPTBN1	spectrin beta, non-erythrocytic 1	11.65618569	4.17E-15
ENST00000025399	STRAP	serine/threonine kinase receptor associated protein	−7.294735531	0.00029061
ENST00000567066	TGFB1I1	transforming growth factor beta 1 induced transcript 1	8.564730191	8.76E-07
ENST00000525962	TGFBR3	transforming growth factor beta receptor 3	8.212151204	5.19E-06
ENST00000576106	TRAP1	TNF receptor associated protein 1	−3.530510601	0.00019337
ENST00000367450	UCHL5	ubiquitin C-terminal hydrolase L5	−7.556237722	0.00012556
ENST00000265428	WWP1	WW domain containing E3 ubiquitin protein ligase 1	−9.115939287	4.09E-08
ENST00000615667	YAP1	Yes associated protein 1	8.212151204	5.19E-06
ENST00000542815	ZEB1	zinc finger E-box binding homeobox 1	9.268512943	1.64E-08
ENST00000392861	ZEB2	zinc finger E-box binding homeobox 2	4.55061543	0.00038525

Table 3.

List of cell adhesion and antioxidant genes along with Ensembl, gene symbol, gene name logFC, p-values in RNA seq data analysis.

Ensembl	Gene Symbol	Gene Name	logFC	p-value
ENST00000553755	LGALS3	galectin 3	8.399184809	2.05E-06
ENST00000619499	FBN2	fibrillin 2	7.294499935	0.00039082
ENST00000559133	FBN1	fibrillin 1	7.294735531	0.00029061
ENST00000599225	LTBP4	latent transforming growth factor beta binding protein 4	7.556237722	0.00012556
ENST00000258733	GPNMB	glycoprotein nmb	7.777534707	4.53E-05
ENST00000454637	CELSR1	cadherin EGF LAG seven-pass G-type receptor 1	7.901380997	2.25E-05
ENST00000200181	ITGB4	integrin subunit beta 4	7.294499935	0.00039082
ENST00000377996	TMEM8B	transmembrane protein 8B	7.629619087	7.45E-05
ENST00000542878	MFGE8	milk fat globule-EGF factor 8 protein	9.623631113	1.90E-09
ENST00000560629	ITGB3	integrin subunit beta 3	7.614824773	9.64E-05
ENST00000403076	SDC1	syndecan 1	7.061890851	0.00072685
ENST00000360134	MAGED4B	MAGE family member D4B	9.175540117	2.87E-08
ENST00000514554	TGFBI	transforming growth factor beta induced	7.744535809	4.53E-05
ENST00000474729	MPZL1	myelin protein zero like 1	7.495170406	0.00016479
ENST00000397857	ITGB2	integrin subunit beta 2	8.013577331	1.45E-05
ENST00000439986	CCBE1	collagen and calcium binding EGF domains 1	5.657885256	2.14E-06
ENST00000218439	MAGED2	MAGE family member D2	2.285685523	0.00330434
ENST00000539168	CDH5*	VE-cadherin	9.90760	3.47E-10
ENST00000262746	PRDX1	peroxiredoxin 1	7.453892	0.000217
ENSG00000165672	PRDX3*	peroxiredoxin 3	7.265215	0.000727
ENST00000470017	PRDX6*	peroxiredoxin 6	8.171648	0.001060

*The protein changes of CDH5, PRDX3, and PRDX6 were validated (Huang et al., 2019)[18].